materials

MDPI

Letter

A New Broadband and Strong Absorption Performance $FeCO_3$/RGO Microwave Absorption Nanocomposites

Wei Huang, Shicheng Wei, Yujiang Wang *, Bo Wang, Yi Liang, Yuwei Huang and Binshi Xu *

National Key Laboratory for Remanufacturing, Academy of Army Armored Forces, Beijing 100072, China

* Correspondence: hitwyj@126.com (Y.W.); xubinshi@vip.sina.com (B.X.); Tel.: +86-010-66718541 (Y.W.); +86-010-66717145 (B.X.)

Received: 30 May 2019; Accepted: 5 July 2019; Published: 9 July 2019

Abstract: A novel composite of $FeCO_3$ nanoparticles, which are wrapped with reduced graphene oxide (RGO), is fabricated using a facile one-spot solvothermal method. The composite consists of a substrate of RGO and $FeCO_3$ nanoparticles that are embedded in the RGO layers. The experimental results for the $FeCO_3$/RGO composite reveal a minimum refection loss (−44.5 dB) at 11.9 GHz when the thickness reaches 2.4 mm. The effective bandwidth is 7.9 GHz between 10.1 and 18 GHz when the refection loss was below −10 dB. Compared to GO and RGO, this type of composite shows better microwave absorption thanks to improved impedance matching. Overall, this thin and lightweight $FeCO_3$/RGO composite is a promising candidate for absorbers that require both strong and broad absorption.

Keywords: $FeCO_3$/RGO; solvothermal method; formation mechanism; microwave absorption properties

1. Introduction

Because of the ubiquity of electronic devices, electromagnetic radiation, and, in particular, signal interference have become a global problem [1–3]. As a result, big efforts have been made to reduce electromagnetic pollution and other related problems. One promising approach is the use of high-performance microwave absorbing materials (MAMs). Graphene, a relatively new carbon-based material, has excellent properties such as high electron mobility, high permittivity and a high specific surface area, which can dampen electromagnetic waves effectively using polarization relaxation [4–7]. However, pure graphene can reflect most of the electromagnetic waves, resulting in being unsuitable for MAM due to their poor impedance matching.

Fortunately, it is possible through to combine graphene with magnetic materials to overcome this problem [8,9]. Most of the related studies are focused on soft magnetic materials, which have high magnetic loss due to natural resonance, and they can produce better results as compounded with graphene. For example, Cui et al. [10] prepared a hollow Fe_3O_4@RGO composite by a facile route. The minimum reflection loss is −41.89 dB at 6.7 GHz. In the range of 1–4 mm, the reflection loss of nanocomposite thickness is less than −10 dB at 3.4 GHz to 13.6 GHz. Wang et al. [11] loaded $MnFe_2O_4$ nanoparticles on RGO sheets by one-step hydrothermal method. The minimum reflection loss of $MnFe_2O_4$/RGO is −32.8 dB at 8.2 GHz with the thickness of 3.5 mm, and the absorption bandwidth with the reflection loss below-10 dB is up to 4.8 GHz (from 7.2 to 12 GHz). Feng et al. [12] synthesized $ZnFe_2O_4$@SiO_2@RGO core-shell microspheres by "coating-coating" method. The minimum reflection loss of the sample with a thickness of 2.8 mm can reach −43.9 dB at 13.9 GHz. In recent years, the composite of paramagnetic $FeCO_3$ and RGO has shown great brilliance in the field of batteries

due to its excellent electrochemical properties [13–15]. However, as far as we know, the microwave absorption properties of $FeCO_3$/RGO, especially its magnetic loss characteristic spectrum, have not been investigated.

Therefore, $FeCO_3$/RGO composites were synthesized using a one-pot solvothermal method. To reveal the microwave absorption mechanism of the $FeCO_3$/RGO composite, the frequency dependence of both complex permittivity and the reflection-loss formation were studied and compared with GO and RGO. The outcome of this study can aid the development of light-weight and broadband electromagnetic-wave absorbers.

2. Experimental

10.8 g $FeCl_3 \cdot 6H_2O$, 7.2 g urea, 5 g PVP and 1.2 g nano-iron powder were added into a 400 mL graphene-oxide slurry (purchased from Qitaihe Baotailong New Materials Co., Ltd. (Qitaihe, China) Containing GO 3.3 mg/mL). The mixture was dispersed, aided by ultrasonic treatment for 30 min, to form a homogeneous solution, and subsequently put into a 500 mL Teflon-lined stainless-steel autoclave, where it was kept at 200 °C for 12 h. After cooling to room temperature, the reaction products were washed with deionized water and alcohol, three times. Finally, the reaction products were dried in a vacuum furnace at 60 °C for 24 h.

The morphology, structure, surface elements, and the electromagnetic parameters were analyzed using SEM, TEM, XRD, XPS, and VNA, field emission scanning electron microscopy (FE-SEM, Nava Nano FE-SEM450/650, Eindhoven, Netherlands), transmission electron microscopy (TEM, LI-BRA200, Oberkochen, German), X-ray diffraction (XRD, D/MAX-2500PC, Rigaku, Tokyo, Japan), X-ray photoelectron spectroscopy (XPS, PHI5300, Ulvac-Phi, Tokyo, Japan), and Vector network analyzer (VNA, PNA-N5244A, AGILENT, Santa Clara, CA, USA),respectively. The electromagnetic parameters of the measured samples were prepared by mixing the products (60%) with molten paraffin wax (40%) and placing them into a toroidal mold (Φ_{in} = 3 mm, Φ_{out} = 7 mm) with a thickness of 2.0–3.0 mm. The test software (AGILENT, Santa Clara, CA, USA) is 85071 and the calibration part is 85050D. Before the test, the permittivity of air was measured as an evaluation of the calibration effect.

3. Results and Discussion

Figure 1a shows the XRD patterns of GO, RGO, and the $FeCO_3$/RGO composite. There is a broad peak at 13.4° in GO (pattern a), which corresponds to the (001) reflection of GO [16]. The broad peak at 25.2° and the disappearance of the peak at 13.4° (pattern b) indicate that GO was reduced to RGO. The XRD patterns of the $FeCO_3$/RGO composite (pattern c) show that all the diffraction peaks match JCPS No.29-0696, which confirms that the $FeCO_3$/RGO composite was indeed obtained. The disappearance of the RGO peaks in $FeCO_3$/RGO [17] due to the uniform distribution of $FeCO_3$ particles between graphene layers (Figure 2), which prevents the interlayer aggregation of RGO sheets, causes the diffraction intensity, i.e., the RGO peak, to be much smaller than for $FeCO_3$.

The XPS survey spectrum of $FeCO_3$/RGO (Figure 1b) shows that the composite consists of Fe, O, C, and N. Four peaks were detected (284.4 eV, 285.8 eV, 287.7 eV, 289.2 eV) in C1s spectrum (Figure 1c), which correspond to C=C/C–C, C–O, C=O, and $FeCO_3$ [13], respectively. As shown in Figure 1d (Fe2p), two peaks appear at 710.1 eV and 723.4 eV, which correspond to $Fe2p_{3/2}$ and $Fe2p_{1/2}$. Furthermore, a satellite peak of $Fe2p_{3/2}$ appears at 714.1 eV [18]. These characteristic peaks confirm the presence of $FeCO_3$/RGO. The formation of $FeCO_3$ can be derived from the following chemical equations:

$$CO(NH_2)_2 + 3H_2O \rightarrow 2NH_4{}^+ + CO_2 + 2OH^- \quad (1)$$

$$CO_2 + 2OH^- \rightarrow CO_3{}^{2-} + H_2O \quad (2)$$

$$2Fe^{3+} + Fe \rightarrow 3Fe^{2+} \quad (3)$$

$$Fe^{2+} + CO_3{}^{2-} \rightarrow FeCO_3 \quad (4)$$

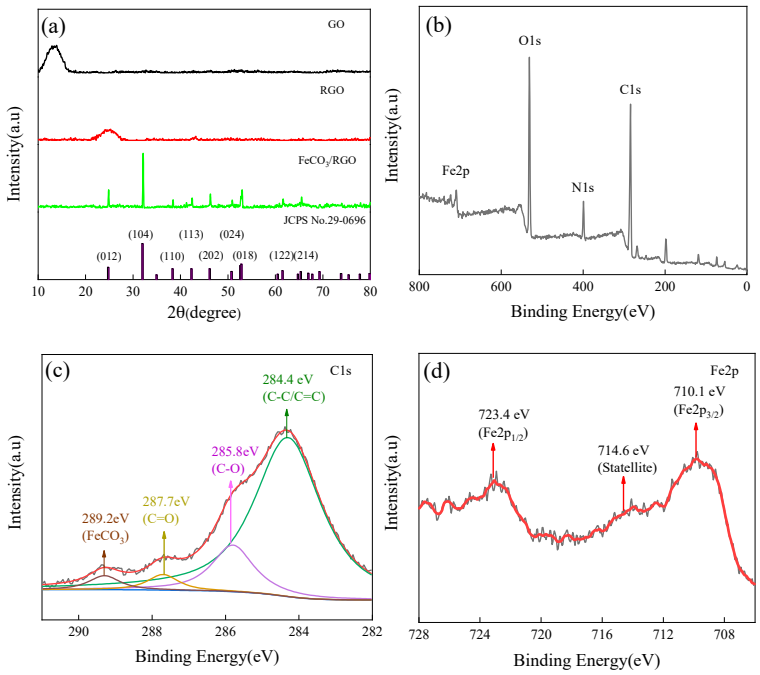

Figure 1. (**a**) XRD patterns for graphene oxide, (GO), reduced graphene (RGO), and $FeCO_3$/RGO; XPS spectra of $FeCO_3$/RGO; (**b**) wide scan; (**c**) C1s spectrum; (**d**) Fe2p spectrum.

Figure 2 shows the SEM, TEM, and HRTEM images of $FeCO_3$/RGO. Polyhedron-like $FeCO_3$ nanoparticles with a diameter of 20~40 nm were evenly embedded in layers of lamellar RGO. The formation of $FeCO_3$ can be also proved by Figure 2c, and the space between two lattice fringes is 0.279 nm, corresponding to (104) plane of $FeCO_3$. During the reduction process, the uniform distributions of nanoparticles in the RGO layers can prevent GO from agglomerating and the formation of a $FeCO_3$-RGO conductive network, which might help facilitate dielectric loss.

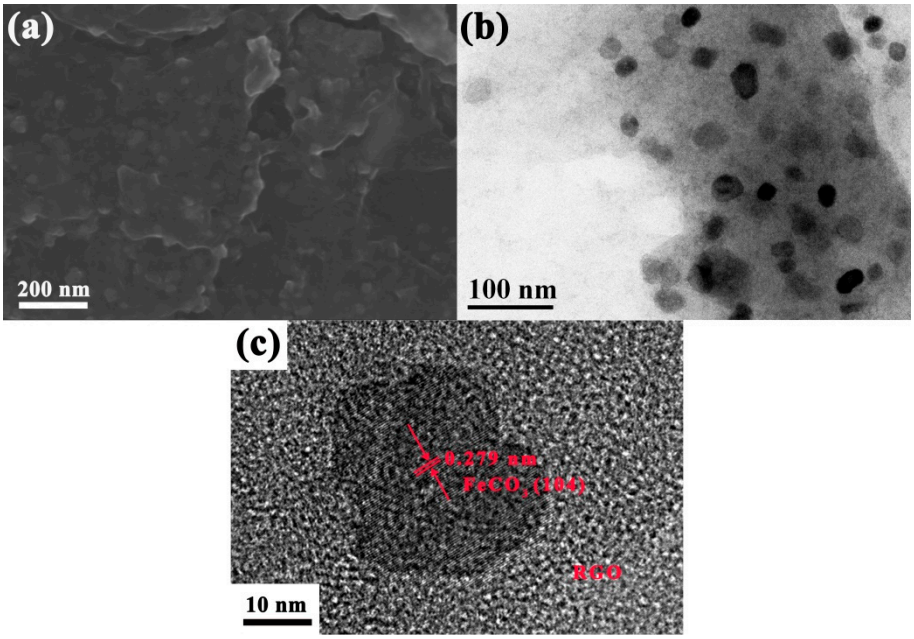

Figure 2. (**a**) SEM; (**b**) TEM; (**c**) HRTEM images of $FeCO_3$/reduced graphene oxide (RGO).

Figure 3 shows the frequency-dependent electromagnetic properties of GO, RGO, and $FeCO_3$/RGO between 2 and 18 GHz. Figure 3a,b illustrate the associated real (ε') and imaginary (ε'') complex

permittivity. The values of ε' show the same trend, ε' decreases with increasing frequency. Furthermore, the ε' of $FeCO_3$/RGO is higher than for both GO and RGO due to the enhanced polarization characteristics. Also, the ε'' of $FeCO_3$/RGO is larger than for both GO and RGO due to higher conductivity [19]. Figure 3c,d depict the real (μ') and imaginary (μ'') complex permeability of the composites. The complex permeability of GO and RGO varies similarly with frequency, indicating that there is little effect of the reduction reaction on the magnetic properties of GO. However, the observed trend for $FeCO_3$/RGO is different from GO and RGO. The complex permeability of $FeCO_3$/RGO varies greatly between 10 GHz and 16 GHz because the magnetic $FeCO_3$ nanoparticles can produce natural resonance loss and exchange resonance loss (due to size effect, surface effect, and spin wave excitation) [20–23].

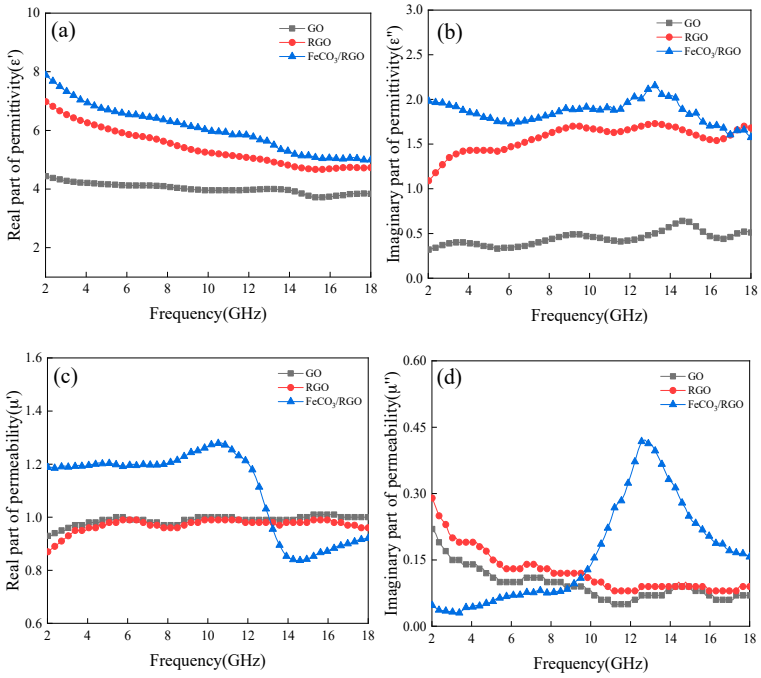

Figure 3. (**a**) ε'; (**b**) ε''; (**c**) μ'; (**d**) μ'' for graphene oxide (GO), reduced graphene oxide (RGO), and $FeCO_3$/RGO.

As well known, reflection loss (R_L) can assess and characterize microwave absorption performance. According to the transmission line model, R_L of a metal-backed microwave absorption layer can be calculated by the following formulas [24]:

$$R_L = 20\lg\left|\frac{Z_{in} - Z_0}{Z_{in} + Z_0}\right| \quad (5)$$

$$Z_{in} = \sqrt{\frac{\mu_r}{\varepsilon_r}}\tanh\left[j\frac{2\pi df}{c}\sqrt{\mu_r\varepsilon_r}\right] \quad (6)$$

Here, Z_{in} is the input impedance of the absorber, Z_0 is the impedance of free space (Z_0 is generally 1), ε_r and μ_r are the complex permittivity and permeability, c is the speed of light in vacuum, d is the thickness of the absorber, and f is the microwave frequency. 3D theoretical R_L plots of the composites are shown in Figure 4a–c. It can be observed that with the reduction of GO and the introduction of $FeCO_3$, the microwave absorption properties improves significantly. $FeCO_3$/RGO nanocomposites show excellent microwave absorption properties as the thickness between 2 mm and 3 mm. R_L curves of composites versus frequency is shown in Figure 4d. $R_{L(min)}$ appears in X and Ku band as thickness in the range of 2–3 mm and shifts to lower frequency with increasing thickness. When the thickness is 2.4 mm, $FeCO_3$/RGO shows optimal microwave absorption and reaches a $R_{L(min)}$ of −44.5 dB, while

the corresponding bandwidth is less than −10 dB is 7.9 GHz (10.1~18 GHz). It is noteworthy that the effective bandwidth of $FeCO_3$/RGO can reach up to 6 GHz and keep steadily when the thickness is 2~3 mm. Table 1 lists some reported microwave absorption composites of soft magnetic based material, graphene-based material, and $FeCO_3$/RGO composite prepared in this work. Notably, $FeCO_3$/RGO composite not only displays a promising negative R_L value, but also has a wide effective absorption bandwidth due to the good impedance matching.

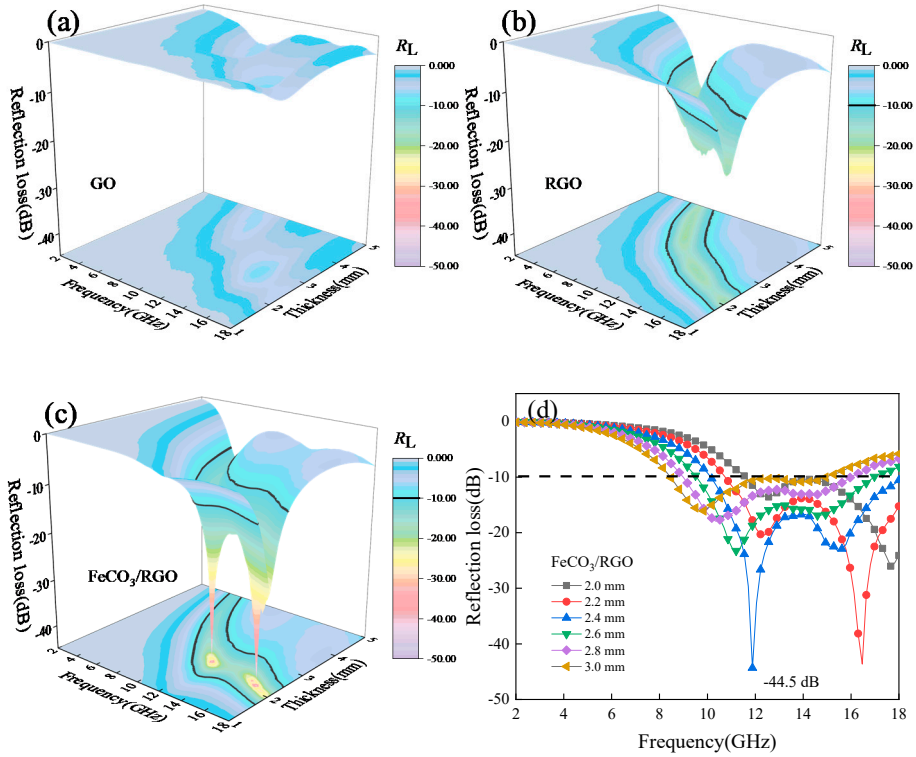

Figure 4. 3D R_L plots of (**a**) graphene oxide (GO); (**b**) reduced graphene oxide (RGO) and (**c**) $FeCO_3$/RGO; (**d**) R_L curves of $FeCO_3$/RGO with 2~3 mm.

Table 1. Microwave absorption performances of the soft magnetic material-based, graphene material-based composite compared with $FeCO_3$/reduced graphene oxide (RGO).

Sample	RL (dB)	Effective Bandwidth (GHz) (RL < −10 dB)	Thickness (mm)	Wt. (%)	Reference
Fe_3O_4/RGO	−41.89	4.2	2.5	50	[10]
Fe_3O_4@SnO_2/RGO	−45.5	3	4.5	50	[25]
$MnFe_2O_4$/RGO	−29	4.88	3	10	[1]
$NiFe_2O_4$/RGO	−58	4.08	2.7	27	[26]
RGO/MWCNTs/$ZnFe_2O_4$	−23.8	2.6	1.5	50	[27]
RGO/MWCNTs/$CoFe_2O_4$	−46.8	3.4	1.6	50	[28]
RGO/Cu_2O/Cu	−51.8	4.1	1.3	50	[29]
CoS_2/RGO	−56.9	4.1	2.2	50	[30]
$FeCO_3$/RGO	−44.5	7.9	2.4	60	This work

4. Conclusions

The $FeCO_3$/RGO composite produced and investigated in this study is a novel material with excellent microwave absorption. The composite can not only effectively facilitate electromagnetic loss but also improve impedance matching. Specifically, the refection loss at 11.9 GHz, when the composite

thickness is 2.4 mm, reaching a minimum of −44.5 dB, and the effective bandwidth is 7.9 GHz (from 10.1 to 18 GHz). In addition, we observed very stable broad characteristics for a thickness range of 2–3 mm. Because of the good properties mentioned above, this composite is can be regarded as an excellent microwave absorber with the potential for many commercial applications.

Author Contributions: W.H., S.W., Y.W. and B.X. designed the experiments, W.H., Y.L. and Y.H. performed the experiments, W.H. and B.W. analyzed the data, W.H., B.W. and Y.W. wrote the paper, B.X. provided theoretical direction.

Funding: This research was funded by the National Natural Science Foundation of China, grant number 51675533 and 51701238.

Conflicts of Interest: The authors declare no conflict of interest.

References

1. Zhang, X.J.; Wang, G.S.; Cao, W.Q.; Wei, Y.Z.; Liang, J.F.; Guo, L.; Cao, M.S. Enhanced microwave absorption property of reduced graphene oxide (RGO)-$MnFe_2O_4$ nanocomposites and polyvinylidene fluoride. *ACS Appl. Mater. Interfaces* **2014**, *6*, 7471. [CrossRef]
2. Radoń, A.; Włodarczyk, P. Influence of water on the dielectric properties, electrical conductivity and microwave absorption properties of amorphous yellow dextrin. *Cellulose* **2019**, *26*, 2987–2998. [CrossRef]
3. Mohammadkhani, F.; Montazer, M.; Latifi, M. Microwave absorption characterization and wettability of magnetic nano iron oxide/recycled PET nanofibers web. *J. Text. Inst.* **2019**, *110*, 989–999. [CrossRef]
4. Plyushch, A.; Zhai, T.; Xia, H.; Santillo, C.; Verdolotti, L.; Lavorgna, M.; Kuzhir, P. Ultra-Light reduced graphene oxide based aerogel/foam absorber of microwave radiation. *Materials* **2019**, *12*, 213. [CrossRef] [PubMed]
5. Chen, Y.; Ma, S.Q.; Li, X.; Zhao, X.; Cheng, X.W.; Liu, J. Preparation and microwave absorption properties of microsheets VO_2 (M). *J. Alloys Compd.* **2019**, *791*, 307–315. [CrossRef]
6. Li, Y.; Li, D.; Yang, J.; Luo, H.; Chen, F.; Wang, X.; Gong, R. Enhanced microwave absorption and surface wave attenuation properties of Co0.5Ni0.5Fe_2O_4 fibers/reduced graphene oxide composites. *Materials* **2018**, *11*, 508.
7. Meng, F.B.; Wang, H.G.; Huang, F.; Guo, Y.F.; Wang, Z.Y.; Hui, D.; Zhou, Z.W. Graphene-based microwave absorbing composites: A review and prospective. *Compos. Part B Eng.* **2018**, *137*, 260–277. [CrossRef]
8. Chen, C.; Xi, J.B.; Zhou, E.Z.; Peng, L.; Chen, Z.C.; Gao, C. Porous graphene microflowers for high-performance microwave absorption. *Nano Micro Lett.* **2018**, *10*, 26. [CrossRef] [PubMed]
9. Yang, Z.W.; Wang, Y.Z.; Xiong, G.Y.; Li, D.; Li, Q.; Ma, C.; Guo, R.; Luo, H. Facile synthesis of $ZnFe_2O_4$/reduced graphene oxide nanohybrids for enhanced microwave absorption properties. *Mater. Res. Bull.* **2014**, *61*, 292–297. [CrossRef]
10. Cui, G.Z.; Liu, Y.L.; Zhou, W.; Lv, X.L.; Hu, J.N.; Zhang, G.Y.; Gu, G.X. Excellent microwave absorption properties derived from the synthesis of hollow Fe_3O_4@reduced graphite oxide (RGO) nanocomposites. *Nanomaterials* **2019**, *9*, 141. [CrossRef]
11. Wang, Y.; Wu, X.M.; Zhang, W.Z.; Huang, S. One-pot synthesis of $MnFe_2O_4$ nanoparticles-decorated reduced graphene oxide for enhanced microwave absorption properties. *Mater. Technol.* **2016**, *32*, 32–37. [CrossRef]
12. Feng, J.T.; Hou, Y.H.; Wang, Y.C.; Li, L.C. Synthesis of hierarchical $ZnFe_2O_4$@SiO_2@RGO core-shell microspheres for enhanced electromagnetic wave absorption. *ACS Appl. Mater. Interfaces* **2017**, *9*, 14103–14111. [CrossRef] [PubMed]
13. Zhang, C.C.; Cai, X.; Xu, D.H.; Chen, W.Y.; Fang, Y.P.; Yu, X.Y. Mn doped $FeCO_3$/reduced graphene composite as anode material for high performance lithium-ion batteries. *Appl. Surf. Sci.* **2018**, *428*, 73–81. [CrossRef]
14. Gu, X.; Yan, C.L.; Yan, L.T.; Cao, L.; Niu, F.E.; Liu, D.D.; Dai, P.C.; Li, L.J.; Yang, J.; Zhao, X.B. Carbonates (bicarbonates)/reduced graphene oxide as anode materials for sodium-ion batteries. *J. Mater. Chem. A.* **2017**, *5*, 24645–24650. [CrossRef]
15. Xu, D.H.; Liu, W.J.; Zhang, C.C.; Cai, X.; Chen, W.Y.; Fang, Y.P.; Yu, X.Y. Monodispersed $FeCO_3$ nanorods anchored on reduced graphene oxide as mesoporous composite anode for high-performance lithium-ion batteries. *J. Power Sources* **2017**, *364*, 359–366. [CrossRef]

16. He, J.Z.; Zheng, Q.C.; Sun, X.; Jin, C.S.; Xi, W.X.; Mao, S.C. Axiolitic ZnO rods wrapped with reduced graphene oxide: Fabrication, microstructure and highly efficient microwave absorption. *Mater. Lett.* **2019**, *241*, 14–17. [CrossRef]
17. Moussa, H.; Girot, E.; Mozet, K.; Alem, H.; Medjahdi, G.; Schneider, R. ZnO rods/reduced graphene oxide composites prepared via a solvothermal reaction for efficient sunlight-driven photocatalysis. *Appl. Catal. B Environ.* **2016**, *185*, 11–21. [CrossRef]
18. Heuer, J.K.; Stubbins, J. An XPS characterization of $FeCO_3$ films from CO_2 corrosion. *Corros. Sci.* **1999**, *41*, 1231–1243. [CrossRef]
19. Lu, M.M.; Cao, W.Q.; Shi, H.L.; Xiao, Y.F.; Jian, Y.; Zhi, L.H.; Hai, B.J.; Wen, Z.W.; Jie, Y.; Mao, S.C. Multi-wall carbon nanotubes decorated with ZnO nanocrystals: Mild solution-process synthesis and highly efficient microwave absorption properties at elevated temperature. *J. Mater. Chem. A.* **2014**, *2*, 10540–10547. [CrossRef]
20. Acher, O.; Gourrierec, P.L.; Perrin, G.; Baclet, P.; Roblin, O. Demonstration of anisotropic composites with tuneable microwave permeability manufactured from ferromagnetic thin films. *IEEE Trans. Microw. Theory Tech.* **1996**, *44*, 674–684. [CrossRef]
21. Wen, F.S.; Yi, H.B.; Qiao, L.; Zheng, H.; Zhou, D.; Li, F.S. Analyses on double resonance behavior in microwave magnetic permeability of multiwalled carbon nanotube composites containing Ni catalyst. *Appl. Phys. Lett.* **2008**, *92*, 04257. [CrossRef]
22. Aharoni, A. Some Recent Developments in Micromagnetics at the Weizmann Institute of Science. *J. Appl. Phys.* **1959**, *30*, S70–S78. [CrossRef]
23. Vleck, V. Concerning the theory of ferromagnetic resonance absorption. *Phys. Rev.* **1950**, *78*, 266–274. [CrossRef]
24. Shu, R.W.; Zhang, G.Y.; Zhang, J.B.; Wang, X.; Wang, M.; Gan, Y.; Shi, J.J.; He, J. Synthesis and high-performance microwave absorption of reduced graphene oxide/zinc ferrite hybrid nanocomposite. *Mater. Lett.* **2018**, *215*, 229–232. [CrossRef]
25. Wang, Y.P.; Peng, Z.; Jiang, W. Controlled synthesis of Fe_3O_4@SnO_2/RGO nanocomposite for microwave absorption enhancement. *Ceram. Int.* **2016**, *42*, 10682–10689. [CrossRef]
26. Zhang, Y.L.; Wang, X.X.; Cao, M.S. Confinedly implanted $NiFe_2O_4$-rGO: Cluster tailoring and highly tunable electromagnetic properties for selective-frequency microwave absorption. *Nano Res.* **2018**, *11*, 1426–1436. [CrossRef]
27. Shu, R.W.; Li, W.J.; Zhou, X.; Tian, D.D.; Zhang, G.Y.; Gan, Y.; Shi, J.J.; He, J. Facile preparation and microwave absorption properties of RGO/MWCNTs/$ZnFe_2O_4$ hybrid nanocomposites. *J. Alloys Compd.* **2018**, *743*, 163–174. [CrossRef]
28. Zhang, K.; Gao, X.; Zhang, Q.; Li, T.; Chen, H.; Chen, X. Preparation and microwave absorption properties of asphalt carbon coated reduced graphene oxide/magnetic $CoFe_2O_4$ hollow particles modified multi-wall carbon nanotube composites. *J. Alloys Compd.* **2017**, *723*, 912–921. [CrossRef]
29. Zong, M.; Huang, Y.; Wu, H.W.; Zhao, Y.; Liu, P.B.; Wang, L. Facile preparation of RGO/Cu_2O/Cu composite and its excellent microwave absorption properties. *Mater. Lett.* **2013**, *109*, 112–115. [CrossRef]
30. Zhang, C.; Wang, B.C.; Xiang, J.Y.; Su, C.; Mu, C.P.; Wen, F.S.; Liu, Z.Y. Microwave Absorption Properties of CoS_2 Nanocrystals Embedded into Reduced Graphene Oxide. *ACS Appl. Mater. Interfaces* **2017**, *9*, 28868–28875. [CrossRef]